

PROTEIN FOLDING AND MODELS OF DYNAMICS ON THE LATTICE

Trinh Xuan Hoang and Marek Cieplak

Institute of Physics, Polish Academy of Sciences, 02-668 Warsaw, Poland

We study folding in 16-monomer heteropolymers on the square lattice. For a given sequence, thermodynamic properties and stability of the native state are unique. However, the kinetics of folding depends on the model of dynamics adopted for the time evolution of the system. We consider three such models: Rouse-like dynamics with either single monomer moves or with single and double monomer moves, and the 'slithering snake' dynamics. Usually, the snake dynamics has poorer folding properties compared to the Rouse-like dynamics, but examples of opposite behavior can also be found. This behavior relates to which conformations act as local energy minima when their stability is checked against the moves of a particular dynamics. A characteristic temperature related to the combined probability, P_L , to stay in the non-native minima during folding coincides with the temperature of the fastest folding. Studies of P_L yield an easy numerical way to determine conditions of the optimal folding.

PACS numbers: 87.15.By, 87.10.+e

Proteins that are found in nature fold rapidly to their native states when physiological conditions are restored^{1,2}. Random sequences of amino acids, on the other hand, may take forever to fold³ or they may have a non-compact ground state. Lattice models have provided insights into the key problems of folding kinetics like the transition through the compactification stage⁴ and existence and characterization of the folding funnel^{5–8}. For the lattice models, the dynamics needs to be declared and there are various ways to define the single step moves for a given Hamiltonian. The time evolution is then implemented by performing a Monte Carlo process or by using the Master equation⁷. One usually adopts the Rouse-like dynamics^{10,11} in which there are two kinds of motions: single- and double-monomer moves. The single-monomer move consists of end-flip and corner moves while the double-monomer move consists of the crankshaft-like rotation. Typically, one declares a certain proportion in which the two kinds of motions are attempted. For instance, one attempts single monomer moves with probability 0.2 and the double monomer moves with probability 0.8¹¹. Chan and Dill⁴ have also studied an expanded set of moves in which a rotation of large segments of the polymer was also allowed.

The thermodynamic stability of a lattice heteropolymer in its native state depends only on the energy spectrum, i.e. on the Hamiltonian, but not on the dynamics itself. The thermodynamic stability may be characterized by the folding temperature, T_f , defined by the value of temperature, T , at which the equilibrium probability to fold, P_0 , is $\frac{1}{2}$. The kinetic propensity to fold may be characterized by T_{min} – the temperature at which the folding process is the fastest, or by the glass transition temperature, T_g , below which the kinetics becomes so slow that folding is kinetically unlikely¹⁵. The definition of T_g relies on the cutoff value of the characteristic folding time whereas T_{min} is defined uniquely and it seems preferable to use the latter. Below T_{min} , an onset of

the glassy effects takes place and the value of T_{min} depends on the dynamics. Here, we demonstrate that this dependence is significant. In particular, we show that a sequence may not even fold if the dynamics is not chosen adequately. Furthermore, we demonstrate that T_{min} is related to the combined probability, P_L , for the sequence to be in non-native local energy minima before finding the native state. Specifically, we show that T_{min} coincides with the temperature at which P_L crosses $\frac{1}{2}$. Notice that whether a given conformation is a local energy minimum or not depends on the set of the dynamics moves used because existence of stability against these moves is what defines a minimum.

We study several heteropolymers on the square lattice and we consider three models of the dynamics: 1) standard Rouse-like dynamics (RD) with the single and double moves applied with the proportions mentioned above, 2) single monomer dynamics (RD1), and 3) the 'slithering snake' dynamics introduced by Wall and Mandel (WMD – for Wall-Mandel dynamics)¹⁴. The latter model imitates snake-like displacement that characterizes motion of polymers in dense solutions and has been introduced as a numerical implementation of the reptation model proposed by De Gennes¹². It is also related to diffusion of a mobile chain through an ordered array of immobile obstacles. Briefly, the dynamics involves choosing randomly one end of the chain and then attempting to advance it to a new neighboring lattice site with the remaining chain following along the previous contour. On the square lattice, both head and tail can attempt to move to three new destinations each. The motion is not allowed if the end site would be occupied by the chain *after* the whole slithering displacement was accomplished. An example of the snake move is represented in Figure 1a. This kind of the dynamics is known¹³ to lead to the well defined $t^{1/4}$ law for the mean square displacement of the central bead, and then to a Rouse-like $t^{1/2}$ law, before the asymptotic diffusive behavior is reached. Here, t denotes

time. Our motivation to consider the snake dynamics is mostly formal – we would like to discuss a dynamics which is clearly distinct from RD. It is conceivable, however, that there may exist sufficiently dense environments in which reptation may turn out to represent the protein motion better.

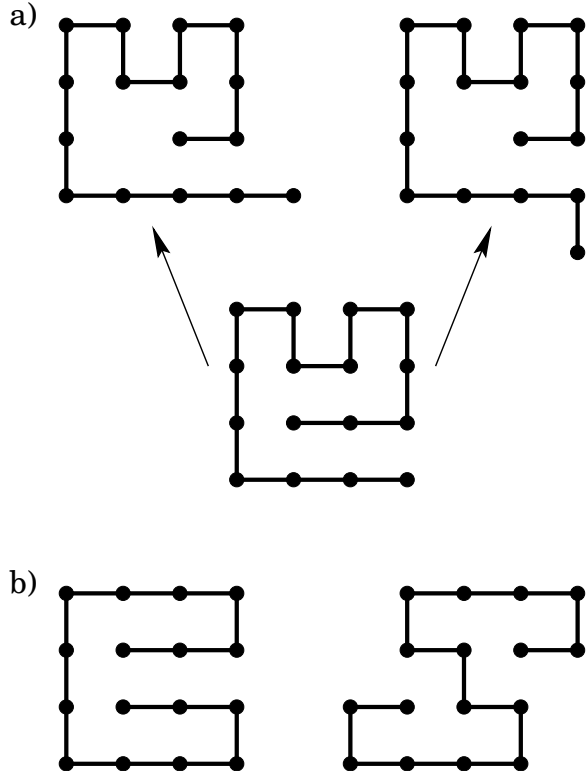


FIG. 1. a) An example of the snake move in WMD: starting from the conformation at the bottom the chain can make a motion either to two adjacent conformations on the top-left and the top-right of the figure. The end bead of the chain finds a new position on the lattice and all the other beads ‘slither’ forward along the previous contour by one lattice constant. Note that the conformation at the bottom is also the native conformation of sequence R. b) Non-ergodicity effects in 16-mer chain: the conformation on the left is not accessible from any other conformation for the move set present in RD, the same thing happens in WMD to the conformation on the right.

Another issue is that of ergodicity. As pointed out by e.g. Chan and Dill⁴, the move set of Rouse-like dynamics is not ergodic for 16-mer chains on the square lattice. We can see this by considering the conformation shown on the left of Figure 1b. This conformation can never be reached by the RD moves but it can by the WMD moves. The conformation on the right of Figure 1b shows a behavior which is just the opposite. For longer chains, non-ergodicity may become significant.

We consider three 16-monomer sequences on the square lattice. Two of them, R and DSKS', have couplings generated with the Gaussian probability distribution and

their values are listed in Ref. 6. Sequence R is constructed by the rank-ordering technique that assigns the most strongly attractive couplings to the native contacts in a target structure⁶. This sequence has been found to be a good folder under the RD⁸. Sequence DSKS', first studied by Dinner et al.⁹, is a bad folder within the same dynamics. We demonstrate that, under WMD, both sequences become bad folders. We then consider an HP-sequence⁴, which we shall encode as HP2, since it has two 2 polar and 14 hydrophobic beads, for which WMD provides better folding than RD. This sequence has the structure H-H-H-H-P-H-H-H-H-H-P-H-H-H-H and the corresponding native state is shown in Figure 2a.

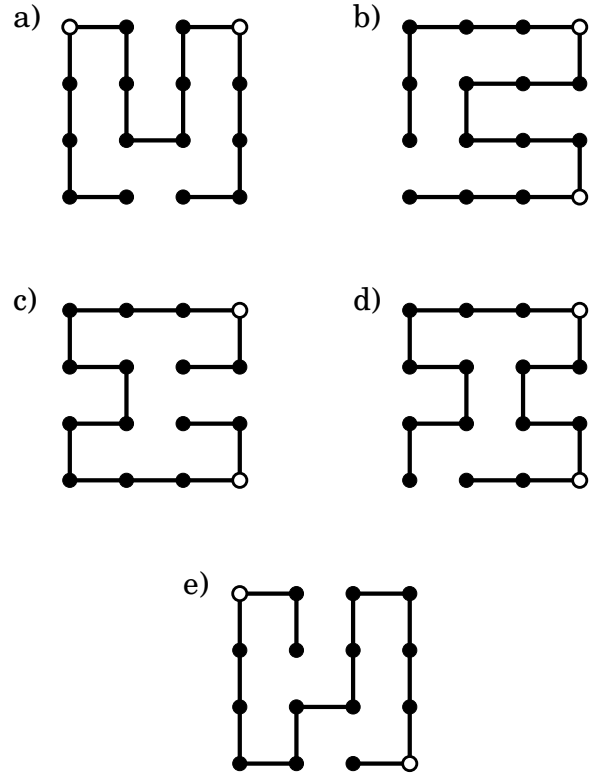


FIG. 2. Native conformations of selected HP sequences with 2 polar beads. The filled and open circles denote hydrophobic (H) and polar (P) amino acids respectively. 2a) corresponds to sequence HP2.

In lattice models, an energy of a sequence in a conformation is given by

$$E = \sum_{i < j} B_{i,j} \Delta(i - j) , \quad (1)$$

where $\Delta(i - j)$ denotes presence of a contact between monomers i and j , i.e. $\Delta(i - j)$ is 1 if indices i and j belong to beads that are nearest neighbors on a lattice but are not neighbors along the sequence. Otherwise, $\Delta(i - j)$ is set equal to 0. $B_{i,j}$ are the corresponding contact energies. Basically, in Gaussian model, $B_{i,j}$ ’s have Gaussian values with a mean shifted by negative

numbers to provide compactness in the ground state. In the HP model² there are only three types of contacts and their energies are $-1, 0, 0$ for the H-H, H-P and P-P pairs respectively. The values of T_f are obtained by an exact enumeration of all conformations and are equal to 1.15, 0.195, and 0.164 for sequences R, DSKS', and HP2 respectively.

Our Monte Carlo simulations have been done in a way that satisfies the detailed balance conditions⁷ and were devised along the lines described in ref.⁴. For polymers, satisfying these conditions is non-trivial because each conformation has its own number, A , of allowed moves that the conformation can make. Thus the propensities to make a move in a time unit vary from conformation to conformation and the effective "activities" of the conformations need to be matched. This can be accomplished by first determining the maximum value of A , A_{max} . For the 16-monomer chain on the square lattice, A_{max} is equal to 18, if the dynamics corresponds to RD or RD1, and 6 in the case of WMD. We associate a single time unit with the conformations in which $A=A_{max}$. This means that each allowed move is being attempted always with probability $1/A_{max}$. For a conformation with A allowed moves, probability to attempt any move is then A/A_{max} and probability not to do any attempt is $1 - A/A_{max}$. The attempted moves are then accepted or rejected as in the standard Metropolis procedure. This description holds for RD1 and WMD. In the case of RD, probability to do a single monomer move is additionally reduced by the factor of 0.2 and to do an allowed double monomer move – by 0.8. The time used in Figures 3-5 is equal to the total number of the Monte Carlo attempts divided by A_{max} . This scheme not only establishes the detailed balance conditions⁷ but it also uses less CPU compared to a process in which moves are attempted with disregard to whether they are allowed or not.

We have carried out Monte Carlo simulations to determine the temperature dependence of the median folding time, t_{fold} , for the three sequences and using the three models of the dynamics. Figure 3 and 4 show the results for R and DSKS' and Figure 5 is for HP2. For each temperature the median folding time is determined based on 200 independent runs starting at random conformations (the cut off is set at value which is significantly above the lowest folding time). The data points shown are averaged over 5 to 10 simulations, each corresponding to 200 trajectories. The figures show that t_{fold} depends on the dynamics in a sensitive way but the temperature dependence of t_{fold} generally has a U-shape with a pronounced minimum (the minimum becomes rather broad only for DSKS' with the RD1). Sequence R is a good folder within RD1 and especially RD but it becomes a bad folder under WMD: T_{min} is significantly above T_f . DSKS' and HP2, on the other hand, are both bad folders for all of the types of dynamics considered here. However, it is interesting to point out that for HP2 the WMD dynamics yields a T_{min} which is comparable to that generated by RD and RD1 and the folding times themselves are sig-

nificantly reduced under WMD. This situation, however, is uncommon: in most cases that we studied, including other HP sequences, except for those shown in Figures 2a - 2d, WMD tends to make the folding poorer. This is because a snake-like move usually breaks many contacts. Sequence HP2 is also uncommon in another respect: it folds better under RD1 than under RD which suggests that for this sequence the crankshaft moves are much less favorable than the single moves.

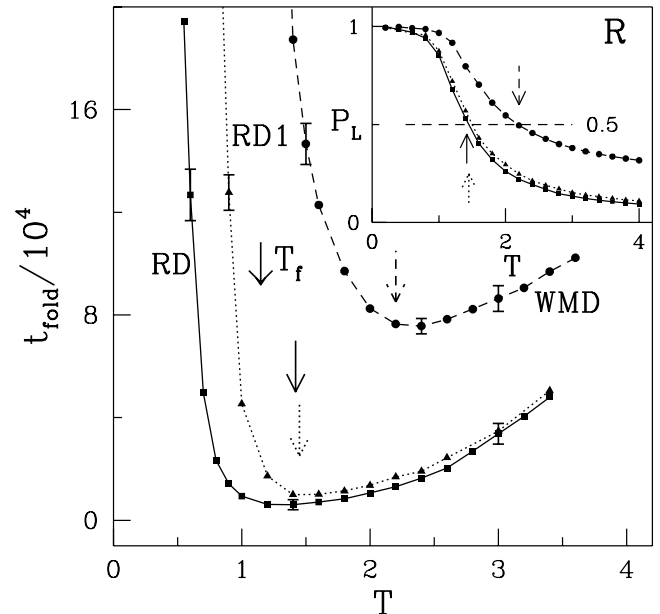


FIG. 3. The median folding time versus temperature for sequence R for the three kinds of the dynamics: RD, RD1 and WMD. The inset shows the temperature dependence of P_L . The arrow associated with T_f indicates the folding temperature. The other arrows indicate temperatures at which P_L crosses 0.5 for each type of the dynamics. Note that they are very close to T_{min} .

The geometry of the native conformation is also an important factor. Generally an HP sequence folds better under WMD than under RD if it has very few polar monomers, but this is not always the case. Figure 2 shows the native states for several HP sequences with 2 monomers of the P-type. The first four of them are fast under WMD but the last one (Figure 2e) is very slow. We have checked that moving out of the native state of Figure 2e by WMD involves a large energy barrier.

It is commonly accepted that folding is a motion that takes place in a rugged energy landscape², which involves crossing many energy barriers. The barriers arise due to the presence of local energy minima (LM) in the system. The role of the minima can be assessed by determining P_L – the probability to encounter LM's on the way to folding. This probability is defined as the fraction of time spent in the LM's relative to the full folding time. This quantity depends on the dynamics explicitly: not only through the definition of what conformation constitutes

a minimum, which could be analyzed by studying the energy spectrum, but also through the fact that the associated weights are not necessarily Boltzmannian. The local minima themselves play a crucial role in some schemes to coarse grain the description of the folding process⁸.

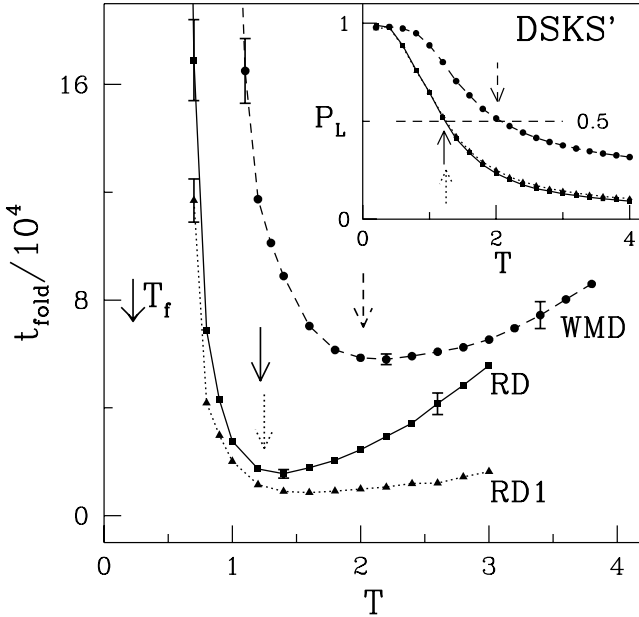


FIG. 4. Same as Figure 3 but for sequence DSKS'.

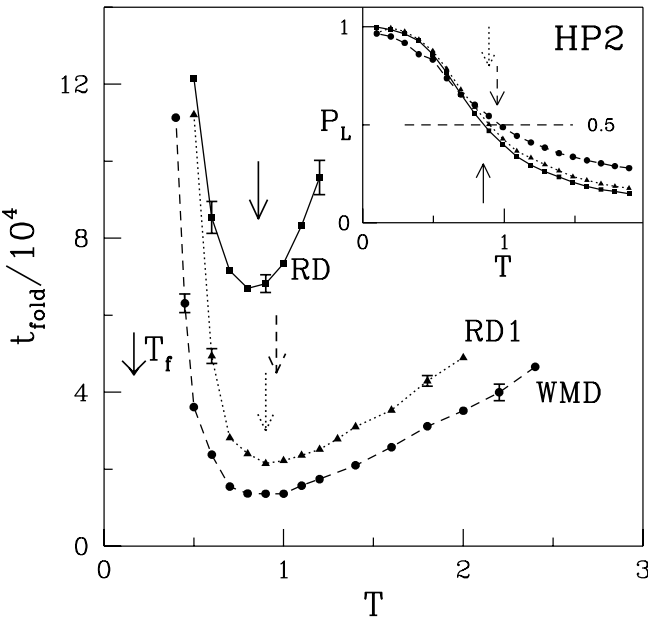


FIG. 5. Same as Figure 3 but for sequence HP2.

There are two kinds of conformations that are LM's: V-shaped, if the energy of the the conformation is lower than the energies of all conformations that are immediately accessible from it, and U-shaped, if one cannot

reach states which are lower in energy but some of the allowed moves leave the energy unchanged. For the 16-mer model there are 802075 possible conformations and only a small fraction, f , of these makes minima. With the RD dynamics, there are 9103 LM's for sequence R out of which 2024 are U-shaped. Each of the U-shaped minima consists of several states thus the total number of states involved in the U-shaped minima is 4893. The total number of states which are minima of whatever kind is then 11972 which makes about $f=1.5\%$ of the phase space. The corresponding numbers for the other sequences and other types of the dynamics are shown in Table I. Checking whether a conformation found on a Monte Carlo trajectory is a local energy minimum or not enhances the CPU by about 50%. An incorporation of the detailed balance conditions already involves an enumeration of the possible moves but checking for the minima requires an additional determination of the resulting energies. Furthermore, checking whether the minimum is U-shaped requires probing possible trajectories within a cutoff number of steps.

Sequence	RD	RD1	WMD
R	11 972 (4 893)	16 425 (8 253)	149 443
DSKS'	12 373 (5 202)	15 851 (7 846)	150 835
HP2	12 606 (5 024)	19 142 (10 093)	103 363

TAB. 1. The total number of conformations that are LM's for each of the sequences for the three kinds of dynamics. The numbers in the brackets correspond to conformations which are in the U-shaped LM's. In case of WMD there are no U-shaped LM's.

For the WMD dynamics, the minima cut out an order of magnitude larger portion of the phase space which alters the energy landscape dramatically. Notice also that when a chain makes a snake move the set of new contacts usually has no overlap with the preceding set of contacts. In the Rouse-like dynamics, on the other hand, the conformations that immediately connect to the native state have sets of contacts which are overlapping to a large extent.

The small fraction of the phase space that corresponds to LM's freezes the kinetics out at $T=0$. Thus at $T=0$ we get $P_L = 1$ whereas at high temperatures P_L is of order f – as shown in Figure 6 for sequence R and DSKS'. There is then a crossover temperature T_L at which P_L crosses $\frac{1}{2}$. Notice that there is no such crossover behavior for the quantity P_L^{eq} which corresponds to P_L with the weights calculated at equilibrium – through the partition function. The reason is that at $T=0$ it is only the native state that has the occupation of 1. Instead, P_L^{eq} has a maximum, which in the case of the sequence R, under RD coincides with T_{min} . In other cases, like for DSKS' as shown in Figure 6, the peak in P_L^{eq} is substantially displaced away from T_{min} towards lower temperatures.

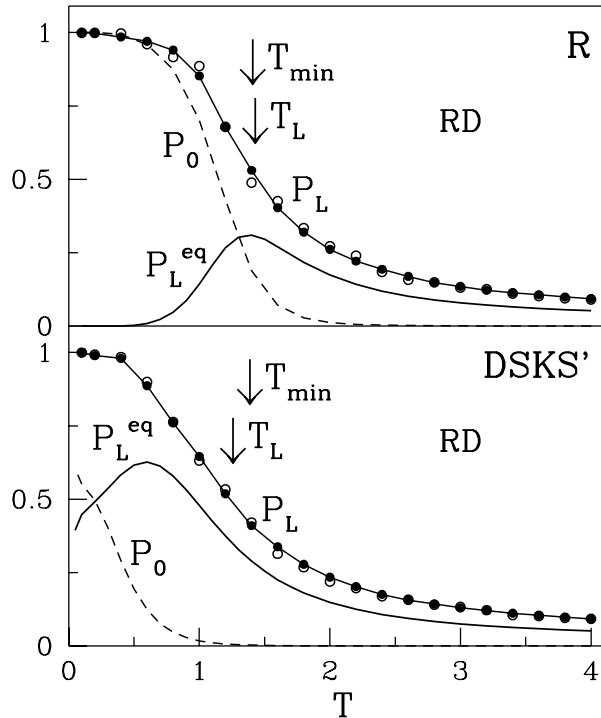


FIG. 6. Plots of P_0 , P_L , and P_L^{eq} vs. temperature for sequence R (top) and DSKS' (bottom) under RD. P_0 and P_L^{eq} are obtained through the exact enumeration of states. The data points for P_L that are marked by the open circles are averaged over 5 MC trajectories whereas those marked by black circles – over 50 trajectories.

The plots of P_L vs. T are shown in the insets of Figures 3, 4, and 5. The data points shown are averaged over 50 trajectories. The striking observation is that T_L appears to coincide with T_{min} for any sequence and for any model of the dynamics that we studied. In other words, folding turns out to be the most favorable at a temperature when half of its time the sequence spends in the local minima during folding. Thus T_L is a measure of temperature below which kinetic trapping in the minima becomes substantial. T_L then conveys the same physics as contained in T_{min} . We have observed that T_L is much easier to calculate than T_{min} because P_L , at any T , converges to a well determined value quite fast: it becomes reliable already after several runs – as demonstrated in Figure 6. For good folders, the temperature at which P_L^{eq} has a maximum is expected to be somewhere around T_f because the maximum signifies an onset of a substantial equilibrium occupation of the native state and the folding funnel dominates the energy landscape. For bad folders, on the other hand, we find that there is essentially no relationship between the temperature of the maximum and T_f because the non-native minima are blocking formation of the native funnel and the position of the maximum is dominated by the nature of the dynamics. The relationship between T_L and T_{min} is well defined both for bad and good folders because the definitions of the two

temperatures are anchored to the dynamics.

In summary, we have shown that the kinetics of folding strongly depends on the details of the dynamics. We have also provided a simplified method to determine the temperature of the fastest folding. The method is based on monitoring the combined occupation of the non-native local energy minima. We have also indicated that, for good folders, the folding temperature can be estimated by studying equilibrium occupation of the minima. Thus the essential characteristics of well folding sequences can be obtained by focusing on the energy minima instead of on the native state itself. This may offer approximate ways to study longer sequences.

We thank for discussions with M. S. Li. This research has been supported by KBN (Grant number 2P03B-025-13).

¹ C. B. Anfinsen, E. Haber, M. Sela, and F. H. White, Proc. Natl. Acad. Sci. U.S.A. **47**, 1309-1314 (1961).

² K. A. Dill, S. Bromberg, S. Yue, K. Fiebig, K. M. Yee, D. P. Thomas, and H. S. Chan, Protein Sci. **4**, 561-602 (1995).

³ C. Levinthal, in *Mossbauer Spectroscopy in Biological Systems*, ed. P. Debrunner (University of Illinois Press, Urbana, 1969).

⁴ H. S. Chan and K. A. Dill, J. Chem. Phys. **99** (3), 2116 (1993); H. S. Chan and K. A. Dill, J. Chem. Phys. **100** (12), 9238 (1994).

⁵ M. Cieplak, S. Vishveshwara, and J. R. Banavar, Phys. Rev. Lett. **77**, 3681-3684 (1996).

⁶ M. Cieplak and J. R. Banavar, Folding & Design **2**, 235-245 (1997).

⁷ M. Cieplak, M. Henkel, J. Karbowski, and J. R. Banavar, Phys. Rev. Lett. **80**, 3654 (1998).

⁸ M. Cieplak and T. X. Hoang, Phys. Rev. E. (in press).

⁹ A. Dinner, A. Sali, M. Karplus, and E. Shakhnovich, J. Chem. Phys. **101**, 1444-1451 (1994).

¹⁰ P. E. Rouse, J. Chem. Phys. **21**, 1273 (1953); A. Baumgärtner in *The Monte Carlo Method in Condensed Matter Physics*, ed. K. Binder (Springer, Berlin, 1995).

¹¹ See also, e.g., A. Sali, E. Shakhnovich, and M. Karplus, Nature, **369**, 248 (1994).

¹² P. G. De Gennes, J. Chem. Phys. **55**, 572 (1971)

¹³ U. Ebert, A. Baumgärtner and L. Schafer, Phys. Rev. Lett. **78** (8), 1592 (1997).

¹⁴ F. T. Wall and F. Mandel, J. Chem. Phys. **63** (11), 4592 (1975); see also J. R. Banavar and M. Muthukumar, Chem. Phys. Lett. **93** (1), 35 (1982).

¹⁵ N. D. Soccia and J. N. Onuchic, J. Chem. Phys. **101**, 1519 (1994).